Development of advanced particle simulation code

Project Representative
Mikito Furuichi Center for Mathematical Science and Advanced Technology, Research Institute for Value-Added-Information Generation, Japan Agency for Marine-Earth Science and Technology

Authors
Mikito Furuichi *[1], Jian Chen*[1], Sota Arakawa*[1], Zhuyuan Lin*[1], Daisuke Nishiura *[1]

*[1] Center for Mathematical Science and Advanced Technology, Research Institute for Value-Added-Information Generation, Japan Agency for Marine-Earth Science and Technology

Keywords: DEM, accretionary prism formation, faulting, earthquake, HPC

1. Introduction

The Discrete Element Method (DEM) solves individual element motions with contact frictions. Large-scale DEM calculations can directly reproduce the multiscale dynamics of granular materials regarding geodynamics, disaster prevention and geotechnical problems. The parallelization of DEM is technically challenging especially for the efficient data management of tangential forces in both shared and distributed memory system. Therefore, we have developed the software DEPTH (DEM based Parallel mulTi-pHysics simulator) for large-scale parallel computing utilizing our original dynamic load balancing technique. In this project, we utilize and improve the DEPTH for various geodynamics, geotechnical and power engineering problems. Here, we introduce the achievements of this FY, regarding the seismic model, geotechnical concrete model, and land slide model developments in the following sections.

2. Energy balance of earthquake in a granular rock box simulation

We performed an energy balance analysis that links seismic focal mechanisms to the development of geological structures in numerical granular rock box experiments, utilizing DEPTH on ES4 [1]. The model simulates the horizontal shortening of a thin 3D granular rock layer on a geological scale (100 km × 0.25 km × 2 km), with a maximum element radius of 12.5 m. This simulation reproduces the millimeter-scale fault displacements caused by the rapid and intermittent motions of elements generating elastic waves, that is, virtual earthquakes. The simulation also captures early postseismic processes, during which popup structure between the active faults is uplifted. Thus, our dynamic energy balance analysis not only illustrated a local shear process but also captured the regional early postseismic deformation processes occurring within several tens of seconds (Fig. 1). Based on changes in the translational kinetic energy, gravitational potential, and both local and regional contact (elastic) potentials, we classified these earthquake processes into three categories: local stress drop generating the primary shock, regional stress release triggered by wave propagation, and structural uplift. Statistical analysis revealed positive correlations between the magnitudes of these representative energy changes and the fault slip. Approximately 0.01% to 60% of the elastic potential energy release of the local fault was converted into wave energy, as estimated by the peak of the translational kinetic energy. The efficiency of this wave energy conversion increased with earthquake magnitude. The increase in gravitational potential, primarily attributed to the uplift of the popup structure, was several orders of magnitude larger than the wave energy. To account for this large gravitational potential change, a local energy balance was deemed inadequate, requiring regional elastic energy changes.

We argue that the inherent diversity of virtual earthquakes in our granular system captures certain aspects of real earthquake behaviors.

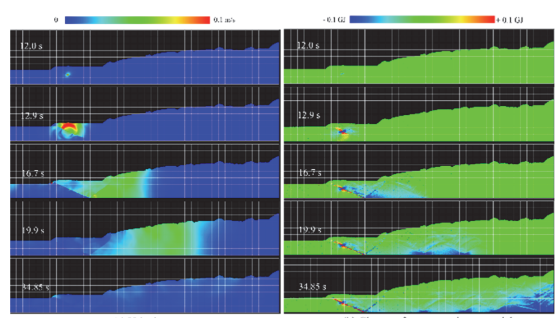

Fig. 1. Visualization of seismic event, depicting changes in (a) velocity and (b) contact potential energy.

3. Flow Simulation of Fiber-Reinforced Concrete

Recently fiber-reinforced concrete has been increasingly used in various structures as a high-performance construction material. By incorporating fiber materials into concrete, tensile strength is enhanced, and cracking and spalling of concrete can be suppressed. Furthermore, by adjusting the material, size, and amount of the fibers according to the intended application, it is possible in some cases to achieve strength comparable to that of reinforced concrete. However, due to their shape, fiber materials tend to orient when flowing together with the fluid. Consequently, during the casting of fiber-reinforced concrete into formwork, fibers may become oriented in specific directions, resulting in anisotropy in the strength of the hardened concrete. In addition, non-uniform distributions of fiber concentration may occur within the concrete. In other words, in order for fiber-reinforced concrete to exhibit the desired performance, it is essential to appropriately control the orientation and distribution of fibers. Nevertheless, the mechanisms governing fiber orientation and distribution in flowing concrete have not yet been fully elucidated, and techniques for controlling fiber behavior have not been established. One of the reasons for this is considered to be the difficulty of experimentally observing fiber behavior in flowing concrete.

In this study, a new viscoplastic force model was introduced into the particle-based simulation software DEPTH to represent interaction forces acting between aggregate particles such as sand and gravel mediated by cement paste, as well as between fiber particles and aggregate particles. Using the discrete element method (DEM), we attempted to develop a model capable of simulating the multiphase flow of concrete and fibers. Casting simulations of fiber-reinforced concrete using DEM were then performed with DEPTH. The orientation and distribution of fibers were compared and validated against previous studies, and the potential of this simulation approach for the optimal control of fiber behavior was examined.

Figure 2 visualizes the flow process of steel fibers and aggregate particles obtained from the casting simulation of fiber-reinforced concrete. As concrete is poured into a rectangular container measuring 150 mm × 150 mm × 1200 mm, the steel fibers can be observed flowing together with the aggregates while undergoing complex rotations and becoming oriented. Figure 3 shows the spatial distribution of steel fibers along the longitudinal direction of the rectangular container after casting. Compared with previous studies(1)(2), the simulation results generally exhibit similar trends; however, quantitatively, there are regions where differences in the amount of steel fibers are observed. Next, Fig. 4 shows the distribution of fiber orientation angles. Here, the orientation angle is defined as the angle between the major axis of a fiber and the longitudinal direction of the rectangular container. While the overall trend of the orientation angle distribution is reproduced, a larger discrepancy from previous studies is observed in the low-angle region. These fiber orientations and distributions are found to depend strongly on the parameters controlling the viscoplastic forces used in the simulation. Therefore, further parameter tuning is required in future work to improve the reproducibility of the simulation results with respect to previous studies.

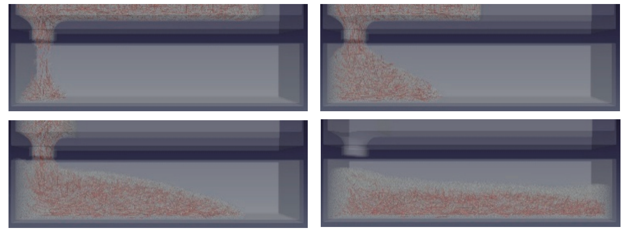

Fig. 2 Snapshots of casting behavior obtained by DEPTH.

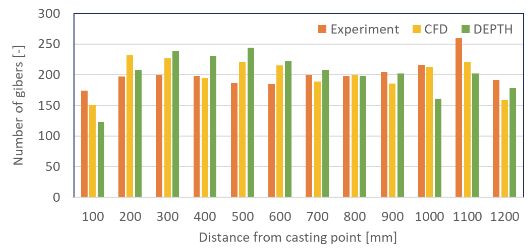

Fig. 3 Horizontal distribution of the number of fibers along the x-axis.

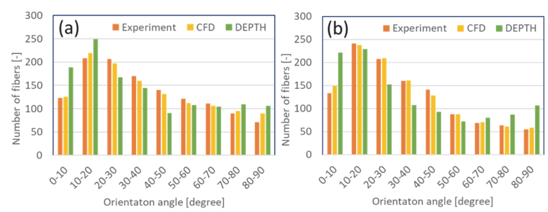

Fig. 4 Inclined angle of fibers in the regions of (a) 0-600 mm and (b) 600-1200 mm of casted beam along the x-axis.

4. Grain-size and mass entrainment in landslide

We adopt DEPTH to model the entire slope as a bonded-particle assembly capable of resolving mass entrainment from particle-scale yielding using ES4. Building on our previous work of Fig. 5, in which we introduced a method for generating erodible slopes from real topographic data, in this study, we systematically investigate the influence of grain size (simulation resolution) on landslide runout dynamics and mass entrainment. The selected results in this section have been presented at DEM10 and submitted as a journal paper currently under review [3].

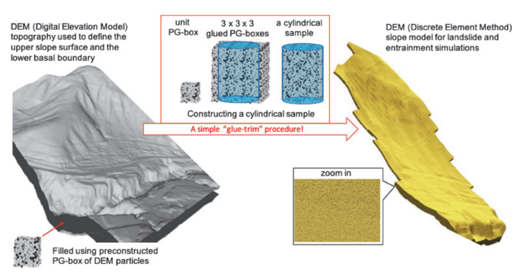

Fig. 5. DEM x DEM modeling method for the 2016 Aso Bridge landslide [2]: Digital Elevation Model from pre- and post-event

used to constrain the bounding surfaces, and boxes constructed with Discrete Element Model particles are used to space-fill the bounded slope.

Using the 2016 Aso Bridge landslide as a case study, we construct DEM slope models based on the pre-event terrain from high-resolution elevation data and simulate the impact of initially released mass for three different particle resolutions under consistent material properties. Tracking the origin of individual particles and quantifying energy transfer allows us to examine how grain size affects the spatial distribution of final deposits and the amount of entrained material, among other observables.

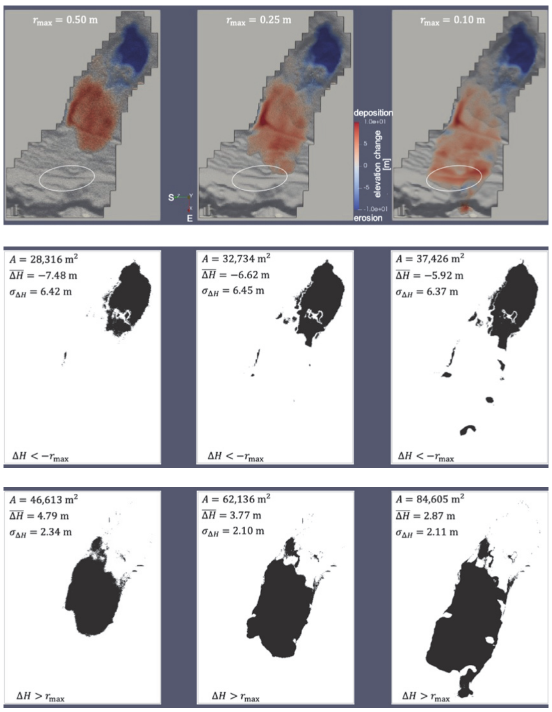

Fig. 6 Final elevation change under three particle resolutions: the affected area A, the mean elevation change $\overline{\Delta H}$, and its standard deviation $\sigma_{\Delta H}$ are listed.

In Fig. 6, we show the dependence of the simulation resolution on the spatial distribution of erosion and deposition. From the figure, it is clearly seen that the runout distance and the lateral spread of mobilized materials both increase with decreasing particle size. In the fine resolution case ($r_{\max} = 0.1$ m), the northern flow front passes over the slope foot and continues to erode the cliff above the Kurokawa River. The southern flow branch also overtops the infrastructure corridor, which roughly corresponds to the secondary failure zone (indicated by the white ellipses). Though it does not fully reach the river in this branch, compared to the actual event. This indicates the need for further increase of simulation resolution (decrease of grain size), which requires a number of grains on the scale of billions. We regard this billion-scale simulation as a future challenge for ES.

In Fig. 7, we present the final travel distance distributions for both released and entrainable materials. Released materials are the particles from the primary failure zone in the crown region of the slope. The entrainable materials are those surrounding the primary failure zone or those in the downstream of the erodible slope. Probability and cumulative distribution functions (PDF and CDF, respectively) of particle travel distance Dt are obtained from the particle counts normalized by the corresponding particle population. From the figure, we can see that the mobility of both released and entrained masses is increased. Particularly, in the entrainable particle group, the fine-resolution case ($r_{\max} =$ 0.1 m) shows a clear rightward shift in both the PDF and CDF, indicating greater and more sustained mobility.

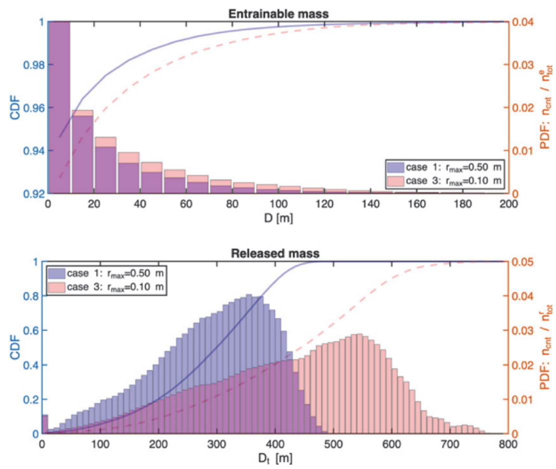

Fig. 7 Probability and cumulative distribution functions (PDF and CDF, respectively) of particle travel distance Dt for released mass and entrainable mass.

Our results demonstrate that grain-scale resolution is a physically meaningful control on landslide mobility and mass entrainment, highlighting the need for considering erodible slope and for fine-resolution landslide simulations. As the next challenge on ES4, we will work on billion-scale DEM landslide simulations.

Acknowledgement

This study was supported by a Grant-in-Aid for Scientific Research (JP24H00279, JP24H01044, JP22H01593, JP22K03789) from the Japan Society for the Promotion of Science (JSPS).

References

[1] M. Furuichi, J. Chen, D. Nishiura , S. Arakawa, R. Arai, D. Sato, and S. Ide, Energy budget analysis of fault motion in a granular rock box simulation, Tectonophysics 908 (2025) 230764

[2] J. Chen, M. Furuichi, D. Nishiura, "Toward large-scale fine resolution DEM landslide simulations: periodic granular box for efficient modeling of excavatable slope", Computers and Geotechnics (165), 105855, 2024

[3] J. Chen, Z.Y. Lin, D. Nishiura, M. Furuichi, “Discrete Element Modeling of Landslides: How Grain Size and Mass Entrainment Affect Runout Dynamics”, under review.